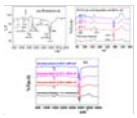

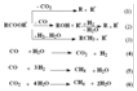

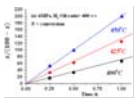

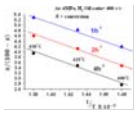

Egyptian Journal of Petroleum

Volume 25, Issue 4, December 2016, Pages 531–537

Full Length Article

Hydrocracking of waste chicken fat as a cost effective feedstock for renewable fuel production: A kinetic study

Samia A. Hanafi, Mamdouh S. Elmelawy, Nasser H. Shalaby , Hussien A. El-Syed, Ghada Eshaq, Mohsen S. Mostafa

Egyptian Petroleum Research Institute, Nasr City, 11727 Cairo, Egypt

Received 10 August 2015, Revised 29 October 2015, Accepted 29 November 2015, Available online 31 December 2015

https://doi.org/10.1016/j.ejpe.2015.11.006

Open Access funded by Egyptian Petroleum Research Institute

Highlights

- Catalytic performances of DHC-8 commercial hydrocracking catalyst were studied in hydrocracking of waste chicken fat.
- Effect of temperatures and LHSV on catalytic conversion and products distribution of waste chicken fat was investigated.
- Periodicity test showed the stability and durability of the catalyst.
- The kinetic study showed that the reaction follows the second order mechanism with an activation energy of 96 kJ mol^{-1}.

Abstract

In this study, low cost waste chicken fat (WCF) feedstock was used for fuel-like hydrocarbon production. The effects of varying reaction parameters on the hydrocracking of waste chicken fat using NiW/SiO_2–Al_2O_3 catalyst were investigated. The reactions were carried out in a fixed bed down flow reactor at reaction temperatures of 400–450 °C, liquid hourly space velocity (LHSV) of 1, 2, 4 h^{-1}, H_2/oil molar ratio of 450 v/v and hydrogen pressures of 6.0 MPa. The effects on hydrocracking conversion and distribution of products were investigated. The liquid product was analyzed using gas chromatography (GC) to quantify *n*-alkanes. Hydrocracking conversion and organic liquid products (OLPs) were evaluated by ASTM D-2887 distillation. The results showed that the catalytic hydrocracking of WCF generates fuels that have chemical and physical properties comparable to those specified for petroleum-based fuels. The amount of kerosene/diesel fractional product decreased with an increase in the temperature and a decrease in the LHSV; while gasoline like petroleum fuel increased. A considerable elimination of O_2 from chicken waste fat molecules has been indicated by FTIR analysis. The oxygen removal pathway of WCF over NiW/SiO_2–Al_2O_3 catalyst is primarily carried

out by hydro-deoxygenation. The reaction was found to follow the second order mechanism, and the estimated activation energy E_a was 96 kJ mol^{-1}. The exploited catalyst was employed in another run where the results showed the catalyst stability and can be used for several times.

Keywords

Hydrocracking; Waste chicken fat; Renewable fuel; Kinetic study

1. Introduction

Demands for energy are increasing and fossil fuels are limited. Research is directed toward alternative renewable fuels [1]; [2] ; [3]. High petroleum prices and the scarcity of known petroleum reserves demand the study of other sources of energy. In this context, agro-industrial wastes (animal and chicken fats, wood, manure …etc.) play an important role as energetic materials. Vegetable oils and fats are basically triglycerides of long-chain fatty acids. The triglycerides have high viscosity which prevents them from being used as fuel in common diesel engines. Therefore, the high viscosity is reduced by the conversion into monoester through the catalytic transesterification reaction for biodiesel production or hydrocarbons are converted by catalytic hydroprocessing for renewable fuel production [4]; [5]; [6] ; [7].

The feedstock issue is the critical point affecting the economic feasibility of biofuel production as it accounts around 80% of the biofuel total cost. In this context, several efforts have been carried out to reduce biofuel prices, essentially by altering lipid sources [8]; [9] ; [10]. Nowadays, edible vegetable oils are the major starting materials for biofuel production. In consequence, prospection for novel feedstocks has been primarily attributed to investigate oleaginous species for inedible oil extraction. Recently, alternatively, lipid residues as waste frying oil, grease, and animal fats have also been receiving considerable attention from the biofuel sector. To take advantage of these low cost and low quality resources, a convenient action would be to reuse residues to integrate sustainable energy supply and waste management in food processing facilities. Poultry fat, with low-cost feedstock compared to high-grade oils, offers another promising feedstock source for biofuel production.

In 2010, chicken fats were the most common and widespread domestic species with an annual consumption of more than 8.6 million tonnes which are persistently growing according to the reports of FAO, of the United Nations. In Europe, the chicken consumption reached 20 kg/capita/year in 2007, according to FAO, while in USA; the chicken consumption has surpassed 50 kg/capita/year, deeming a mature chicken to weight 1.8–1.9 kg (1.5 of meat) [8]. Then a larger amount of waste fats from chicken processing-plants has been generated in countries. Within agro-industrial residues chicken fats may be used to solve inappropriate environmental disposal besides contributing to energy supply. Many studies investigated the availability of chicken fats for biodiesel production by transesterification [11]; [12]; [13] ; [14]. Chicken fat was thermally treated in the presence of mono-functional acid catalysts by Tian et al. [15] in a pilot scale two-stage fluid catalytic cracking reactor. In another work, the same authors [16] examined the behavior of chicken fat at different temperatures with different catalysts (USY, HZSM-5, Al_2O_3 and SiO_2) in a fixed bed reactor, where they observed a high conversion rate using acid catalysts (USY and HZM-5). Scarce works have been devoted to investigate systematically the hydrocracking process of chicken fat using bi-functional catalysts (hydrogenation-dehydrogenation and acid functions) as sulfided $NiW/SiO_2–Al_2O_3$ catalyst.

This work focused on the effect of process parameters (temperature, and LHSV) on the hydrocracking of waste chicken fat to renewable fuel production to be in comparison with our previous study for WCO hydrocracking over the same catalyst [17].

2. Experimental

2.1. Materials

Waste chicken fat (WCF) feedstock was obtained from Koki Company for poultry shop products and services-Cairo, Egypt. DHC-8 commercial distillate-hydrocracking catalyst is provided by UOP.

Prior to analysis, waste chicken fat was filtered for impurities removal and then, heated with stirring for 3 h at 110 °C to remove moisture.

2.2. Characterization

2.2.1. Waste chicken fat characterization

The elemental composition of WCF was determined using an elemental analyzer with channel control model (Pw 1390-Philips) and spectrometer model Pw 1410. Fatty acid content in WCF was analyzed using an Agilent 6890N FID-GC with an Omnistar Q-mass, HP-624 Capillary column was used (Table 1). The physical characterizations of WCF feedstock were measured according to the American Society for Testing and Materials (ASTM) methods (Table 2).

Table 1.
Composition of WCF feedstock.

Elemental composition, wt.% (ASTM D4294-90)				
Carbon	Hydrogen	Nitrogen	Sulfur	Oxygen
74.9	12.73	0.08	0.008	12.28

Species of fatty acids in WFC feedstock, wt.%						
C14:0	C16:0	C16:1	C18:0	C18:1	C18:2	C18:3
0.3	21.0	4.5	5.0	38.0	31.0	0.2

Table options

Table 2.
Physical characterization of WCF feedstock.

Properties	Value	Standard methods
Density (20 °C) (kg/m^3)	921	ASTM D4052-91
Refractive index (70 °C)	1.4602	ASTM D 1747-09
Pour point (°C)	7	ASTM D2500
Acid value (mg KOH/g-oil)	4.5	ASTM D664
Flash point (°C)	213	ASTM D93
Viscosity (40 °C) (mm^2/S)	50	ASTM D445
Iodine value (g I_2/100 g)	70	ASTM D1959-97

Table options

2.2.2. Catalyst characterization

DHC-8 is a hydrocracking catalyst consisting of non-noble hydrogenation metals (NiO–WO_3) on an amorphous silica alumina support. Physicochemical properties were obtained from UOP; BET surface area and pore volume were determined by N_2 adsorption–desorption at −196 °C from linear BET plots using Micrometrics Gimini 2375 surface area analyzer, USA, while pore volume was determined by poresizer 9320-V_2-08, USA. The measurement was performed on sample heated at 200 °C for 2 h in pure nitrogen. The main properties of the catalyst are shown in Table 3.

Table 3.
Physicochemical properties of DHC-8 catalyst (after Hanfi et al. [17]).

Texture properties		Physical properties			Chemical composition (wt.%)		
BET surface area (m^2/g)	Pore volume	Size (mm)	Shape	Bulk density compacted (kg/m^3)	Alumino-Silicates	WO_3	NiO

	(cc/g)							
				Dense	Sock, v			
239	0.36	1.6	Sphere	743.3	704.8	85–95	5–15	<2

Table options

2.2.3. Hydrocracking activity test

Hydrocracking of WCF was performed in a fixed bed down flow tubular reactor of 100 cm^3 effective volume (L = 50 cm, ID = 1.6 cm). Prior to the hydrocracking reaction, the catalyst was activated with cyclohexane-dimethyldisulfide (DMDS, 2 wt.%) as a sulfiding reagent, with a flow rate of 150 ml/min under 3.0 MPa hydrogen pressure and reaction temperature 260 °C for 3 h, and then 360 °C for another 3 h. After catalyst activation, the reactor was cooled to room temperature, pressurized with H_2 to 6 MPa hydrogen pressure, and then heated to the desired temperature. After reaching the desired reaction conditions, WCF and hydrogen were introduced into the reactor at 6 MPa hydrogen pressure, a fixed liquid hourly space velocity (LHSV) of 4, 2, or 1 h^{-1}, and a H_2/oil molar ratio of 450 v/v. The liquid and gaseous products were collected for analysis.

2.2.4. Analysis of products

The product mixtures obtained from hydrocracking of WCF were separated to gas phase, water and liquid organic products (LOPs) where Agilent 7890A GC instrument, USA, was used for all chromatographic measurements.

The composition of the gaseous products was analyzed using two detectors, Thermal Conductivity Detector (TCD) for analysis of non-organic gases, which were separated in a 7 ft Hysep Q, molecular sieve packed stainless steel column, and a Flam Ionization Detector (FID) for C_1-C_5 hydrocarbon separation in a 60 meter (Capillary) DB-1 silicon oil fused silica by using helium at 50 °C and 5 min hold. Injector and detector temperatures are 150 °C and 250 °C, respectively.

The hydrocarbon composition of the liquid organic products were analyzed to quantify *n*-alkanes, and to make a relative comparison of hydrocarbon distributions, using FID and 30 m (Capillary) Hp-5. The column temperature was programed as: 50 °C for 10 min rise to 300 °C at the rate of 4 °C/min and nitrogen carrier gas flow was 1 ml/min. Unconverted triglycerides, viz., the starting materials, as well as oxygenated intermediate products were measured using INNO WAX 60 m, 320 μm ID, and film thickness 250 μm. The hydrocracking reaction conversion and gasoline/kerosene/diesel yield were evaluated by distillation. The atmospheric distillation up to 180 °C was carried out according to the ASTM D 2887 standard. The vacuum distillation of the atmospheric distillation residue was carried out according to the ASTM D1160. The liquid organic products (LOPs) are classified into three distillated fractions: (i) C_5–C_8 fractions distillated at 65–150 °C, are defined as alkanes ranging of naphtha; (ii) C_9–C_{14} fractions, obtained at 150–250 °C which is the range of kerosene; (iii) C_{15}–C_{18} fractions, obtained at 250–340 °C, diesel range, and the residue >340 °C which are unconverted triglycerides starting materials, as well as oxygenated intermediate products.

The feed conversion is calculated by the following equation:

Turn on

where X_{feed} and $X_{product}$ are the weight percent of the unconverted feedstock (oxygenated intermediate at temperature >340 °C), and the weight percent of products, respectively [14].

The yield of the target fraction was calculated using the following equation:

Fourier transform infrared (FTIR) spectroscopy (ATI Mattson Infinity series apparatus Model 960 Moo9, USA) was used to investigate the chemical composition of OLPs and follow up the progress of fat conversion.

3. Results and discussion

3.1. FTIR analysis

Fig. 1 shows the spectra of waste chicken fat feedstock, petroleum fractions (gasoline, kerosene/diesel and hydrocracked products) obtained at chosen operating conditions using NiW/SiO_2–Al_2O_3 catalyst. The spectra appear to be prevalently aliphatic hydrocarbons as evidenced by the appearance of the intense C–H stretching bands of alkanes in the 3008–2854 cm^{-1} region and aliphatic C–H bending of methyl and methylene groups at 1377 and 1462 cm^{-1} respectively. The absorption peak at 722 cm^{-1} suggested the out of plane bending of alkene. As WCF feedstock is mainly triglycerides, the CO group gives rise to a strong absorption at 1744 cm^{-1} which is a representative of glyceride ester. The absorption peak at 1722 cm^{-1} is assigned as fatty acids. Also, the bands at 1163, 1170 and 1241 cm^{-1} are corresponding to the presence of C–O– of ester. Hydrocracking of WCF leads to the production of n-alkanes and a decrease in oxygenated compound peaks. The extent of this conversion varies according to operating conditions. In addition, the pronounced diminution of the peak intensity of alkene (CC) around 725 cm^{-1} confirms the procession of the double bond saturation involved in fat molecules.

Figure 1.
FT-IR spectra of waste chicken fat feedstock and products of its hydrocracking as a function of different reaction parameters in comparison to the corresponding petroleum products.

Figure options

3.2. Catalytic conversion

3.2.1. Variation of temperature

The effect of reaction temperature on hydrocracking of waste chicken fat (WCF) was studied in a fixed-bed reactor using NiW/SiO_2–Al_2O_3 catalyst. The experimental results were examined in terms of conversion %, yield % of liquid organic product (LOP), and gaseous and aqueous phases. Table 4 shows that the conversion of WCF increases steadily with the increase in reaction temperature. The highest conversion was 99.5 wt.% at 450 °C, 6.0 MPa and 1 h^{-1}, which may fit with the IR spectra (Fig. 1). The LOP yield % decreases significantly with the increase in reaction temperature at a fixed LHSV and operating pressure due to the higher rate of cracking in accordance to [1]; [15] ; [16]. This

indicates that a major fraction of WCF has suffered a secondary cracking, resulting in the formation of a gaseous product. Methane, ethane, propane, and butane, were major compounds of the gaseous products. Propane represented the largest wt.% in the gaseous products as it is the common denominator in all possible pathways [17], but C_3H_8 content decreases with the increase in reaction temperature (Table 4) which may be attributed to the exothermic hydrodeoxygenation (the main producer for propane) at higher temperature is thermodynamically unfavorable [18]. As the reaction temperature increases, the increase in CH_4 and C_2H_6 content may be due to the hydrogenolysis of triglyceride hydrocarbon products [19]. It should be recalled here that either CO or CO_2 could not necessarily be observed (if they are formed), as the catalyst could be active enough for the water–gas shift (WGS) equilibrium and methanation of CO and CO_2 in presence of hydrogen and water vapor [20]. It is evident that the loss of LOP yield had an impact on the yield of the kerosene/diesel products where the gasoline range fraction yield increases with the increase in reaction temperature (Table 4).

Table 4.
Effect of reaction temperature on hydrocracking of waste chicken fat feedstock as a function of LHSV (pressure = 6 MPa, H_2/oil = 450 vol./vol.).

LHSV, h^{-1}		4			2			1		
Temperature (°C)		400	425	450	400	425	450	400	425	450
Conversion (wt.%)		94	97	98.1	97	98.4	99	98.5	99.2	99.5
Residual fats (wt.%)		6	3	1.9	3	1.6	1.0	1.5	0.8	0.5
Products distribution (wt.%)	Gaseous	12.8	20.5	22.7	15.7	23.0	24.7	18.3	24.1	26.0
	OLP	78.8	70.5	68.7	76.5	69.9	68.6	74.8	68.7	66.5
	Aqueous phase	2.4	6.0	6.7	4.8	5.5	5.7	5.4	6.5	7.0
OLP composition, wt.%	Naphtha 45/80 °C	25.8	32.5	35.7	31.2	35.4	40.6	43.3	47.2	49.5
	Kerosene/diesel 180/400 °C	53	38.0	33.0	45.3	34.5	28.0	31.5	21.5	17.0
Gaseous state composition at selected conditions, wt.%	Methane	1.3	3.8	5.5	2.0	–	–	3.5	–	–
	Ethane and ethylene	1.0	5.2	6.9	2.7	–	–	4.6	–	–
	Propane and propylene	**9.5**	**8.5**	**7.3**	**9.0**	–	–	**7.2**	–	–
	Butanes	1.0	3.0	3.0	2.0	–	–	3.0	–	–

Propane is the largest wt% in the gaseous products.

Table options

Since chicken fat is mainly triglyceride, its deoxygenation is predicted to proceed along three pathways, decarboxylation (DCO_2), decarbonylation (DCO), and hydrodeoxygenation (HDO), by which the oxygen content of triglyceride is converted to CO_2, CO, and water, respectively [19] ; [20]. These byproducts and other lighter hydrocarbons bring about a mass loss of the yield of LOP. According to the deoxygenation reaction pathway shown in Scheme 1, one mole of C_n (where *n* signifies the carbon number) fatty acid in the triglyceride generates a C_n hydrocarbon by hydrodeoxygenation (pathway 3) with two moles of hydrogen consumed, but generates a C_{n-1} hydrocarbon by decarbonylation (pathway 2) or decarboxylation (pathway 1) with one mole of hydrogen consumed or no hydrogen consumed, respectively.

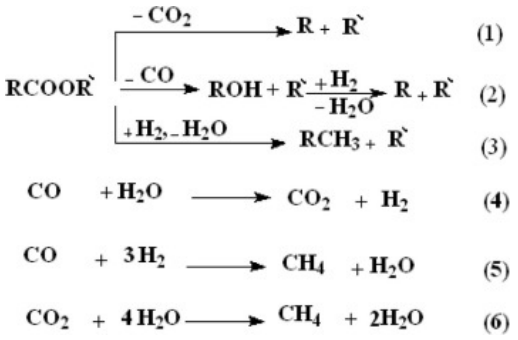

Scheme 1.
Possible reaction pathways for the hydroprocessing of triglyceride.

Figure options

On the way of triglycerides deoxygenation, C–C bond scission leads to the oxygen removal forming CO_2 or CO as a byproduct, whereas C–O bond scission produces H_2O. Two additional reactions, water gas shift (Eq. (4)) and methanation (Eqs. (5 and 6)) are also needed to be considered due to the formation of CO_2 and CO [14] ; [18]. NiW/SiO_2–Al_2O_3 bi-functional catalyst (containing hydrogenation sites and acid sites) may be responsible for the enhanced hydrodeoxygenation reaction [21] ; [22]. To investigate the relative activities of decarboxylation/decarbonylation and hydrodeoxygenation, the ratio of C_{15} and C_{17} to C_{16} and C_{18} in the liquid product can serve as an indicator of the relative activities, because the WCF used in this study composed mainly of C_{16} and C_{18} fatty acids (Table 1). As Table 5 shows, the C_{15+17}/C_{16+18} ratios in the liquid product were less than unity and decreased with the increase of temperature, indicating that the deoxygenation pathway over NiW/SiO_2–Al_2O_3 catalyst is mainly hydrodeoxygenation. This result is also in agreement with the results obtained from the yield of water.

Table 5.
Effect of reaction temperature on OLPs composition as a function of LHSVs for selected samples (pressure = 6 MPa, H_2/oil ratio = 450 v/v).

LHSV (h^{-1})		**4**			**2**	**1**
T (°C)		400	425	450	400	400
n-Alkanes ⩽ C_8 (yield, wt.%)		**25.8**	**32.5**	**35.7**	**31.2**	**43.3**
Kerosene (165–240 °C) C_9–C_{14}	C_9–C_{14} (wt.%)	**40**	**29**	**28.6**	**38.5**	**28.4**
	C_9	4	7.5	9.2	10.7	11.6
	C_{10}	6	4.7	5.4	7.7	6.0
	C_{11}	6.2	5.0	5.1	7.0	5.4
	C_{12}	12	5.6	4.6	8.1	3.8
	C_{13}	7.7	4.5	3.0	3.6	1.2
	C_{14}	4.1	1.7	1.3	1.4	0.4
Diesel (240–340 °C)	C_{15}–C_{18} (wt.%)	**30.9**	**21.2**	**11**	**16.8**	**7.6**
	C_{15}	6.4	4.5	0.93	0.8	0.6
	C_{16}	12.8	9.0	4.4	8.3	3.5
	C_{17}	4.0	2.5	1.4	1.0	0.9
	C_{18}	7.7	5.2	4.3	6.7	2.6
	C_{15} + C_{17}/C_{16} + C_{18}	0.51	0.50	0.3	0.12	0.23
	>340 °C, C_{19+}	**1.9**	**1.0**	**0.6**	**0.6**	**0.54**

Table options

Table 4 shows that the product distribution of LOPs varies greatly with temperature. The kerosene/diesel yield (C_9–C_{18}) hydrocarbons dramatically decrease with the increase of temperature probably due to the successive cracking reaction of the long chain paraffins, while gasoline yield (<C_9) increases with temperature. The catalytic cracking reaction is

the selective C–C scission of the carbonyl carbon and adjacent alpha-carbon to it in a triglyceride molecule [23]. It is a direct route to the hydrocarbon chains of fatty components of the triglycerides. Hence, it is the most ideal and also the shortest route at arriving to short chain hydrocarbon [24]. Due to the strong cracking activity of $NiW/SiO_2–Al_2O_3$ catalyst, it is not considered as the suitable choice for long-chain alkane production ($C_{15–18}$), but it is a good catalyst choice for naphtha-like hydrocarbon production in accordance to [20].

3.2.2. Effect of LHSV

As can be seen in Table 4, an overall decrease trend for conversion of WCF (i.e., the less effective deoxygenation) is observed with an increase in LHSV. This was caused by the shorter (not sufficient) retention time. A high LHSV would suppress the cracking reactions, which was confirmed by Table 4 ; Table 5. The $\leqslant C_8$ yield decreases but the yields of $C_9–C_{18}$ increase with the increase in LHSV. Therefore, increasing LHSV will cause relatively a higher kerosene/diesel fraction yield due to less cracking. As shown in Table 5 the C_{17} and C_{18} yields have a similar behavior, which indicates that the effect of LHSV on HDO and DCO/DCO_2 reactions has no significant difference [24].

3.3. Kinetics study

Fig. 2 allows us to determine the reaction order of the catalytic hydrocracking of WCF over sulfided $NiW/SiO_2–Al_2O_3$ catalyst, at different temperatures, namely, 400, 425, and 450 °C. The linear kinetic plots of the conversion of WCF to OLPs, obtained with reaction time up to 1 h, under the assigned operating conditions (LHSV of 1, 2 and 4 h^{-1}, 6.0 MPa operating pressure, and 400 v/v H_2/oil ratio), fit well with the second-order mechanism [25] ; [26]. Moreover, the dependence of the reaction rate constants (k_2) derived from Fig. 2, on the temperature is represented by the Arrhenius equation as:

$$\ln k_2 = \ln A - E_a/RT$$

where A is the frequency factor, E_a is the apparent activation energy, R is the universal gas constant, and T is the absolute reaction temperature (Fig. 3). The estimated activation energy for the reaction under the mentioned conditions was 96 kJ mol^{-1}.

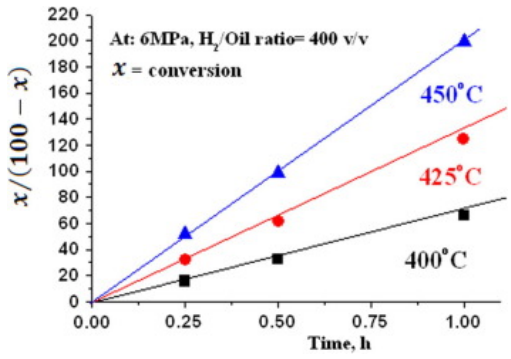

Figure 2.
Plot of conversion (x) versus time of reaction for various temperatures.

Figure options

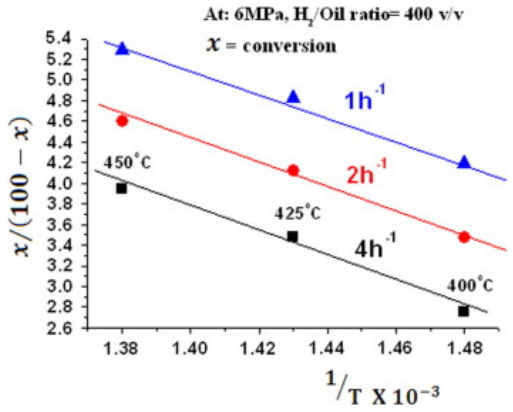

Figure 3.
Arrhenius plots for hydrocracking of WCO at 6 MPa, 375–450 °C, for various LHSV.

Figure options

3.3. Periodicity test

Of special interest from the application point of view, the exploited catalyst (NiW/SiO_2–$Al_2O_3)_{Re}$ was employed in another run. The conversion and oil liquid products (OLPs) were taken as a probe for the catalytic performance. The activity was investigated at LHSV of 1 and 4 h^{-1} with the same conditions of the first run, Table 6. The activity seems to be the same of the fresh catalyst, indicating the stability and reusability of the catalyst for several times.

Table 6.
Effect of reaction temperature on hydrocracking of waste chicken fat feedstock over the exploited catalyst (NiW/SiO_2–$Al_2O_3)_{Re}$ as a function of LHSV (pressure = 6 MPa, H_2/oil = 450 vol./vol.).

LHSV (h^{-1})	4			1		
Temperature (°C)	400.0	425.0	450.0	400.0	425.0	450.0
Conversion (wt.%)	94.2	96.7	98.4	98.3	99.1	99.4
Residual fats (wt.%)	5.8	3.3	1.6	1.7	0.9	0.6
OLPs	76.8	71.5	67.4	73.6	69.1	64.9

Table options

4. Conclusion

The effects of varying processing parameters on the production of hydrocarbons from waste chicken fat over NiW/SiO_2–Al_2O_3 catalyst were investigated. With the increase in the reaction temperature and decrease in the LHSV, the hydrocracking conversion, degree of oxygen removal, and *n*-paraffin yields tended to increase where gasoline fraction increased and the amount of kerosene/diesel decreased. Due to the strong cracking activity of NiW/SiO_2–Al_2O_3 catalyst, it is not considered as the suitable choice for long-chain alkanes (C_{15-18}), but it is a good catalyst choice for naphtha fraction. The reaction was found to follow the second order mechanism with an activation energy of 96 kJ mol^{-1} as concluded from the kinetics study. The activity results of the exploited catalyst (NiW/SiO_2–$Al_2O_3)_{Re}$ were within the range of those of the original catalyst.

References

[1] J.E. Gay
Joint Force Q., 73 (2014), pp. 44–51 2nd Quarter
Loading

[2] J.A. Melero, G. Calleja, A. Garcia, M. Clavero, E.A. Hernandez, R. Miravalles, T. Galindo
Fuel, 89 (2010), pp. 554–562
Loading

[3] E. Sannita, B. Aliakbarian, A.A. Casazza, P. Perego, G. Busca
Renew Sust Energ Rev., 16 (2012), pp. 6455–6475

Loading

[4] B. Veriansyah, J.Y. Han, S.K. Kim, S.A. Hong, Y.J. Kim, J.S. Lim, Y.W.S. Oh, J. Kim
Fuel, 94 (2011), pp. 578–585
Loading

[5] K. Murata, Y. Liu, M. Inaba, I. Takahara
Energy Fuels, 24 (2010), pp. 2404–2409
Loading

[6] A. Ishihara, N. Fukui, H. Nasu, T. Hashimoto
Fuel, 134 (2014), pp. 611–617
Loading

[7] S.D. Darunde, D.M. Mangesh
Int. J. Emerg. Technol. Adv. Eng., 2 (2012), pp. 179–186
Loading

[8] M.A. Abdoli, F. Mohamed, B. Ghobadian, E. Fayyazi
Int. J. Environ. Res., 8 (2014), pp. 139–148
Loading

[9] A. Wisniewski Jr., V.R. Wiggers, E.L. Simionatto, H.F. Meier, A.A.C. Barros, L.A.S. Madureira
Fuel, 89 (2010), pp. 563–568
Loading

[10] G.P. McTaggart-Cowan, S.N. Rogak, S.R. Munshi, P.G. Hill, W.K. Bushe
Fuel, 89 (2010), pp. 752–759
Loading

[11] T.B. Emaad, B.F. Abdelrahman, J. Pak
Anal. Environ. Chem., 12 (2012), pp. 95–102
Loading

[12] H.N. Bhatti, M.A. Hanif, M. Qasim, A. Rehman
Fuel, 87 (2008), pp. 2961–2966
Loading

[13] A. Ertan, C. Mustafa, S. Huseyin, World Renewable Energy Congress-Sweden, 13–18 May 2011, pp. 319–324.
Loading

[14] J.K. Satyarthi, D. Striniras
Energy Fuels, 25 (2011), pp. 3318–3322
Loading

[15] H. Tian, C. Li, C. Yang, H. Shan
Chin. J. Chem. Eng., 16 (2008), pp. 394–400
Loading

[16] Id
Chin. J. Catal., 29 (2008), pp. 69–76
Loading

[17] S.A. Hanafi, M.S. Elmelawy, H.A. El-Syed, N.H. Shalaby
J. Adv. Catal. Sci. Technol., 2 (2015), pp. 27–37
Loading

[18] Y.K. Ong, S. Bhatia
Energy, 35 (2010), pp. 111–119
Loading

[19] E. Rasmus, M. Niels, S. Lars, Z. Per
PTQ Q2, Q2 (15) (2010), pp. 101–106
Loading

[20] I. Kubičková, D. Kubička
Waste Biomass Valorization, 1 (2010), pp. 293–308
Loading

[21] Y. Liu, R.S. Boyás, K. Murata, T. Minowa, K. Sakanishi
Catalysts, 2 (2012), pp. 171–190 http://dx.doi.org/10.3390/catal2010171
Loading

[22] G.W. Huber, P.O. Connor, A. Corma
Appl. Catal. A, 329 (2007), pp. 120–129
Loading

[23] P. Adewale, M.J. Dumont, M. Ngadi
Renew. Sust. Energy Rev., 45 (2015), pp. 574–588
Loading

[24] T.M. Sankaranarayanan, M. Banu, A. Pandurangan, S. Sivasanker
Bioresour. Technol., 102 (2011), pp. 10717–10723
Loading

[25] W. Charusiri, T. Vitidsant
Energy Fuels, 19 (2005), pp. 1783–1789
Loading

[26] D. Leckel
Energy Fuels, 22 (2008), pp. 231–236
Loading

Peer review under responsibility of Egyptian Petroleum Research Institute.

Corresponding author.